

Stability of Discrete Integration Algorithms for a Real-Time, Second-Order System

R. E. McFarland

NASA, Ames Research Center

October, 1997

Real-time implementations of damped, second-order systems are examined in terms of stability of the discrete realizations. In this analysis the required double integration is separated, because nonlinearities are assumed to accompany the outputs of each discrete integration algorithm. For example, “anti-windup” limiters may be assumed in a control system application, as shown in the Laplace representation given by Fig. 1.

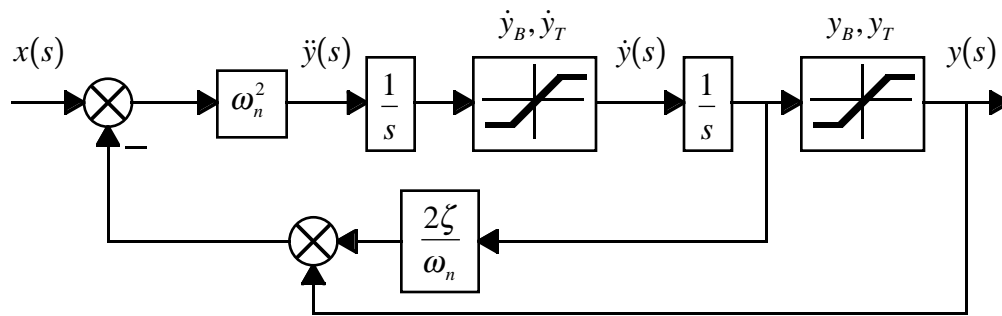


Fig. 1 - Laplace Representation

If the discrete implementation of a second order system is to be stable, it must be stable in linear regions, when nonlinearities are not encountered. For this reason, the linear discrete system is analyzed. In the case of limiters, the phenomenon of encountering a nonlinearity on either integration reduces the order of the system, and this implies stability if the discrete implementation of the second-order system is stable. The entrance to, and exit from nonlinear regions constitute boundary value problems.

The stability of a discrete implementation depends on the system parameters, and on the selected integration algorithms. In this analysis, the maximum possible cycle time h is determined for each algorithm, as required to maintain stability in the discrete implementation. A particular high frequency system (called the “target system”) is periodically mentioned, where the natural frequency ω_n is given as 75 rad/sec, the damping is $\zeta = 0.7$, and the cycle time $h = 0.025$ seconds. For this taxing discrete model, where the duty cycle $\omega_n h = 1.875$, it is shown that none of the discrete algorithms are capable of producing a stable discrete realization.

The linear, conventional second order system representing the linear form of Fig. 1 may be diagrammed in z-transform space using symbolic integration operators as follows:

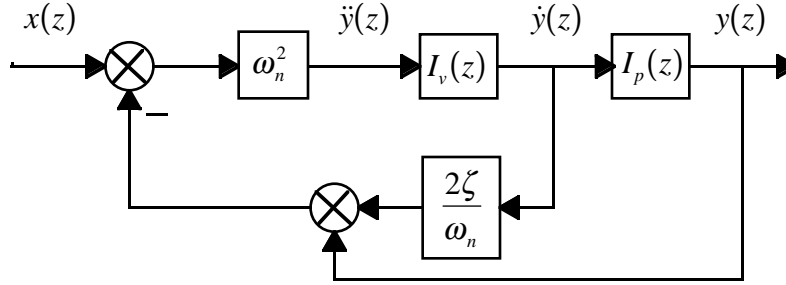


Fig. 2 - Linear, Discrete Representation

The Algorithms

In order to recursively solve the differential equation representing the second-order system, the acceleration \ddot{y}_k is computed from the current input x_k , and the states y_k and \dot{y}_k which have been predicted from the preceding recursion.

$$\ddot{y}_k = \omega_n^2 x_k - 2\zeta\omega_n \dot{y}_k - \omega_n^2 y_k$$

Any mixed combination of subscripts in this equation produces an erroneous mathematical statement. From the acceleration (and possibly using the previous value of the acceleration \ddot{y}_{k-1}), five different algorithmic combinations are selected in this analysis. The individual integration algorithms considered are (1) Euler, an explicit algorithm which is called Rectangular in its implicit form, (2) Adams-Bashforth 2nd, which is an explicit algorithm, and (3) Trapezoidal, which is an implicit algorithm, but also used as an explicit form herein when required to satisfy the recursion. These algorithms pretty much exhaust the possibilities for real time simulation work, which requires low-order, causal algorithms. The combinations selected are assumed to (1) advance the time index of the velocity, and (2) create the advanced position from this velocity. These combinations are:

- (1) ET - The Euler algorithm to create the velocity from the acceleration, known to advance the time index by only half a time step (h), followed by the Trapezoidal (or Tustin, or Triangular, or Adams-Moulton 2nd order) algorithm, known to preserve the time index, to create the position from the velocity.
- (2) ER - The Euler algorithm (explicit) to create the velocity from the acceleration, followed by the Rectangular algorithm (implicit) to create the position from the velocity. In this algorithmic combination the velocity tends to be advanced a half time step, and the position then tends to be advanced by the full time step.
- (3) TT - The Trapezoidal algorithm in an advancing form to create the velocity from the acceleration, followed by the Trapezoidal algorithm to create the position from the velocity. This sequence is what Engineers get when they insist on using the Tustin algorithm for both integrations.
- (4) AT - The Adams-Bashforth 2nd order integration (explicit) algorithm to create the velocity from the acceleration, followed by the Trapezoidal algorithm (implicit). In this algorithmic combination, widely used at Ames Research Center's simulation facilities for low frequency aircraft states, the velocity tends to be advanced a full time step, and the position is then concurrent with the velocity.

- (5) AR - The Adams-Bashforth 2nd order integration (explicit) algorithm to create the velocity from acceleration, followed by the Rectangular algorithm (implicit). In this algorithmic combination the velocity tends to be advanced a full time step, and the position tends to be advanced an additional half time step.

The time shifts inherent in the individual integration algorithms, as mentioned above, are modified in the discrete implementation as a function of the feedback terms. This complex interaction influences the stability of the discrete system, and none of the combinations can uniformly advance the states of the system over the entire range of frequencies. Dependent upon the system parameters, some algorithms have better performance than others.

Analysis Relationships

The position output of the second-order discrete system is related to its input by the *closed-loop* system function of Fig. 2,

$$\frac{y(z)}{x(z)} = \frac{I_v(z)I_p(z)\omega_n^2}{1 + 2\zeta\omega_n I_v(z) + \omega_n^2 I_v(z)I_p(z)} = \frac{F(z)}{1 + F(z)G(z)}$$

and this representation reveals the *open-loop* system (by breaking the feedback path),

$$H(z) = F(z)G(z) = \omega_n I_v(z) [2\zeta + \omega_n I_p(z)]$$

which is used to determine stability properties. The gain and phase of the open-loop system will be displayed, as a function of the various integration algorithms.

For the display of time responses, the velocity of the closed-loop system is used:

$$\frac{\dot{y}(z)}{x(z)} = \frac{I_v(z)\omega_n^2}{1 + 2\zeta\omega_n I_v(z) + \omega_n^2 I_v(z)I_p(z)}$$

The time response of the velocity of the closed-loop system displays stability problems more readily than does the position. Indeed, for some algorithms, short time-period observations of just the position response conceals the fact that the velocity may be divergent. Note that the open-loop system is identical for both position and velocity, so the frequency-domain stability analysis is robust. For the target system, the desired closed-loop time response of the velocity to a unit step input is given in Fig. 3.

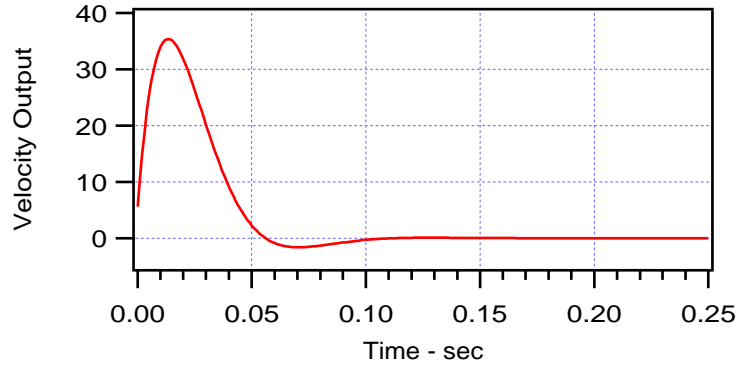


Fig. 3 - Desired Velocity Response

In order to examine the stability of the discrete second order system, the open loop transfer function is evaluated at the *phase crossover frequency*, defined as the point where the phase angle of $H(z)$ is $-\pi$. At this point the *gain margin* is defined as:

$$\text{gain margin} = |H(z)|^{-1} \text{ when } \phi(z) = -\pi$$

If the gain margin is less than or equal to unity, the system is unstable. This also means that $H(z)$ is outside the unit circle. The *phase margin* is defined as how much the phase is above $-\pi$ when the gain margin is unity. If the phase margin is not above this value, then the system is also unstable.

Note that the closed-loop Laplace function,

$$\frac{y(s)}{x(s)} = \frac{\frac{\omega_n^2}{s^2}}{1 + \frac{\omega_n}{s} \left(2\zeta + \frac{\omega_n}{s} \right)}$$

produces the open-loop Laplace function,

$$h(s) = \frac{\omega_n}{s} \left(2\zeta + \frac{\omega_n}{s} \right)$$

with phase angle given by,

$$\phi = \tan^{-1} \left(\frac{2\zeta\omega}{-\omega_n} \right)$$

such that the initial phase angle (as $\omega \rightarrow 0$) begins its response in frequency space at the value of $-\pi$. Phase angles produced in the material given below using z-transforms are adjusted to reflect this fact.

For the “target system” the desired gain and phase of the open-loop system $h(s)$ are shown in Figs. 4(a) and 4(b).

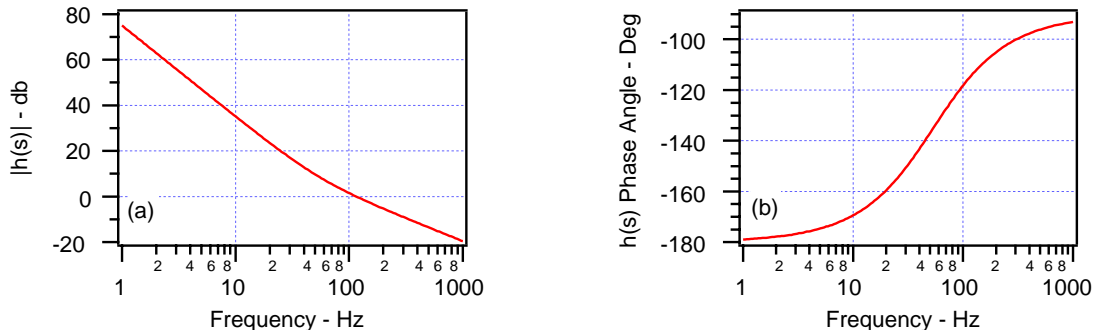


Fig. 4 - Desired Open-Loop Performance

For comparison purposes, these curves are reiterated on other performance figures. The five different algorithmic combinations are analyzed in Appendices A through E.

Analysis Results

As a function of the system damping, the algorithmic combinations produce the following results in terms of stable discrete processes. The required duty cycle $\omega_n h$ is produced as a function of the system damping.

Algorithm	Program Sequence	Damping	For Stability
ET	$\dot{y}_{k+1} = \dot{y}_k + h\ddot{y}_k$	$\zeta < 1/2$	$\omega_n h < 4\zeta$
	$y_{k+1} = y_k + \frac{h}{2}(\dot{y}_{k+1} + \dot{y}_k)$	$\zeta \geq 1/2$	$\omega_n h < 1/\zeta$
ER	$\dot{y}_{k+1} = \dot{y}_k + h\ddot{y}_k$ $y_{k+1} = y_k + h\dot{y}_{k+1}$	All	$\omega_n h < 2(\sqrt{1+\zeta^2} - \zeta)$
TT	$\dot{y}_{k+1} = \dot{y}_k + \frac{h}{2}(\ddot{y}_k + \ddot{y}_{k-1})$ $y_{k+1} = y_k + \frac{h}{2}(\dot{y}_{k+1} + \dot{y}_k)$	All	$\omega_n h < (1 + 2\zeta^2 - \sqrt{1 + 4\zeta^4})/\zeta$
AT	$\dot{y}_{k+1} = \dot{y}_k + \frac{h}{2}(3\ddot{y}_k - \ddot{y}_{k-1})$	$\zeta < 1/\sqrt{12}$	See Footnote ¹
	$y_{k+1} = y_k + \frac{h}{2}(\dot{y}_{k+1} + \dot{y}_k)$	$\zeta \geq 1/\sqrt{12}$	$\omega_n h < 1/(2\zeta)$
AR	$\dot{y}_{k+1} = \dot{y}_k + \frac{h}{2}(3\ddot{y}_k - \ddot{y}_{k-1})$ $y_{k+1} = y_k + h\dot{y}_{k+1}$	All	$\omega_n h < 2(\sqrt{\zeta^2 + \frac{1}{2}} - \zeta)$

Table I - Stability Analysis Results

This material is also presented in graphical form in Fig. 5. For each of the integration combinations, the discrete model is unstable if the duty cycle is above the pertinent curve.

¹ Damping must satisfy $\zeta \geq \frac{\sqrt{9\omega_n^4 h^4 + 8\omega_n^2 h^2 + 16} - 4 - \omega_n^2 h^2}{8\omega_n h}$

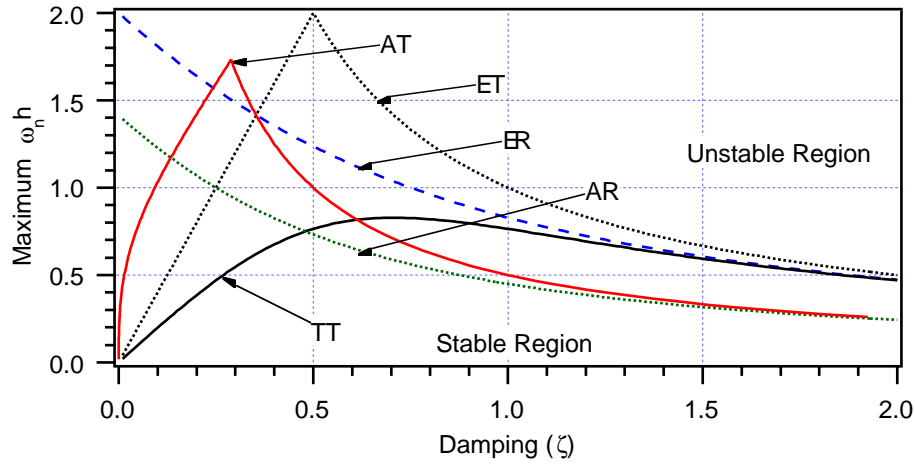


Fig. 5 - Stability Boundaries

For the target system, where $\omega_n h = 1.875$ and $\zeta = 0.7$, none of the algorithms produces stability. For this system, where $\omega_n = 75$ rad/sec, the maximum possible cycle time is given in Fig. 6.

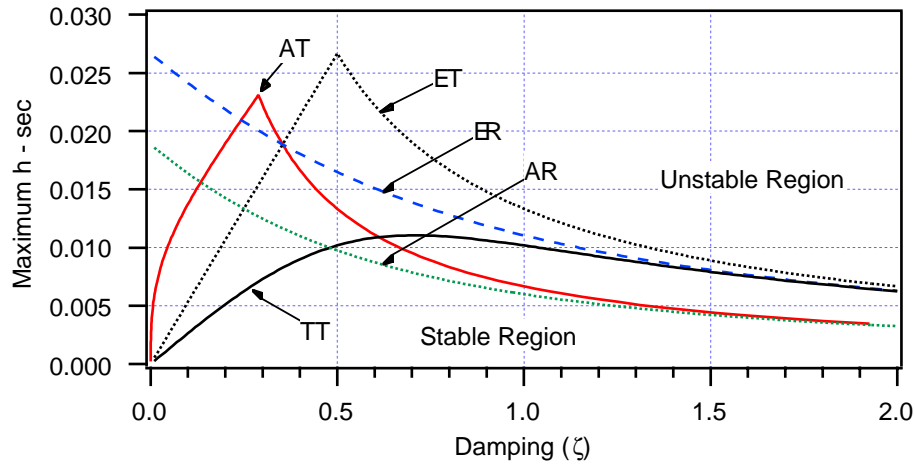


Fig. 6 - Target System Maximum Cycle Time

For stability using the target system, the maximum cycle times are presented in Table II.

Algorithm	Maximum h - sec
ET	0.01905
ER	0.01388
TT	0.01104
AT	0.00952
AR	0.00787

Table II - "Target System" Stability Limits

From Table II we see that none of the algorithmic combinations are capable of solving the target system.

Conclusions

Due to the stability boundaries developed here, the selection of an appropriate integration sequence for a system with a high natural frequency requires a careful choice. For example, a “target system” (representing a real actuator problem) has recently been presented to our simulation facility, and this system is too fast to be solved using an array of possible algorithms.

Although it appears that a multi-rate procedure is the only solution to the target system (with accompanying aliasing problems), a project has recently been completed where an alternate algorithmic approach successfully solves the target system. This technique will soon be published.

Appendix A

Euler-Trapezoidal (ET)

Using Euler integration for the acceleration-to-velocity integral followed by trapezoidal integration for the velocity-to-position integral produces the following code fragment for a second order system,

$$\ddot{y}_k = \omega_n^2 x_k - 2\zeta\omega_n \dot{y}_k - \omega_n^2 y_k$$

$$\dot{y}_{k+1} = \dot{y}_k + h\ddot{y}_k$$

$$y_{k+1} = y_k + \frac{h}{2}(\dot{y}_{k+1} + \dot{y}_k)$$

which may be written in z-transform notation by,

$$\ddot{y}(z) = \omega_n^2 x(z) - 2\zeta\omega_n \dot{y}(z) - \omega_n^2 y(z)$$

$$\dot{y}(z) = \frac{h}{z-1} \ddot{y}(z)$$

$$y(z) = \frac{h(z+1)}{2(z-1)} \dot{y}(z)$$

Hence, for the Euler-Trapezoidal set, the symbolic integrations are given by,

$$I_v(z) = \frac{h}{z-1}$$

$$I_p(z) = \frac{h(z+1)}{2(z-1)}$$

The closed-loop system for the velocity is given in z-transform notation by,

$$\frac{\dot{y}(z)}{x(z)} = \frac{\frac{h\omega_n^2}{z-1}}{1 + \frac{2\zeta\omega_n h}{z-1} + \frac{h^2\omega_n^2(z+1)}{2(z-1)^2}}$$

and in order to investigate the stability properties, we examine the open-loop function,

$$H(z) = \frac{2\zeta\omega_n h}{z-1} + \frac{h^2\omega_n^2(z+1)}{2(z-1)^2} = \frac{h\omega_n}{2(z-1)^2} [(h\omega_n + 4\zeta)z + h\omega_n - 4\zeta]$$

which has a phase angle given by,

$$\phi = \tan^{-1} \left[\frac{(4\zeta - \omega_n h) \sin \omega h}{(\omega_n h + 4\zeta) - (4\zeta - \omega_n h) \cos \omega h} \right] - \pi$$

As $\omega h \rightarrow \pi$ (the Nyquist frequency), the phase margin vanishes. At this frequency, where $z = -1$, the system magnitude is given by,

$$|H(-1)| = \zeta \omega_n h$$

The system is unstable if $|H(z)| > 1$ (outside the unit circle). Thus for stability the cycle time must conform to the inequality,

$$h < \frac{1}{\zeta \omega_n}$$

Also, if $4\zeta < \omega_n h$, then $\phi \leq -\pi$, and the system is unstable.

For a stable system we thus have $1 > \zeta \omega_n h$, and if $4\zeta < \omega_n h$, the combination of these inequalities produces $\zeta = 1/2$. Hence, in the region of lower damping, where $4\zeta < \omega_n h$, for stability the cycle time must conform to the inequality,

$$h < \frac{4\zeta}{\omega_n}$$

These two inequalities produce a piecewise continuous curve, where the smallest inequality is required for stability. For a stable Euler-Trapezoidal algorithm we thus have,

$$h < \begin{cases} \frac{4\zeta}{\omega_n} & \zeta < \frac{1}{2} \\ \frac{1}{\zeta \omega_n} & \zeta \geq \frac{1}{2} \end{cases}$$

Using the given damping and frequency parameters for the target system, the Euler-Trapezoidal scheme is unstable for cycle times above 0.019 seconds. At this cycle time, the magnitude and phase are shown in Figs. A1(a) and A1(b). Considerable deterioration is shown in phase, as compared to the desired phase of Fig. 4(b).

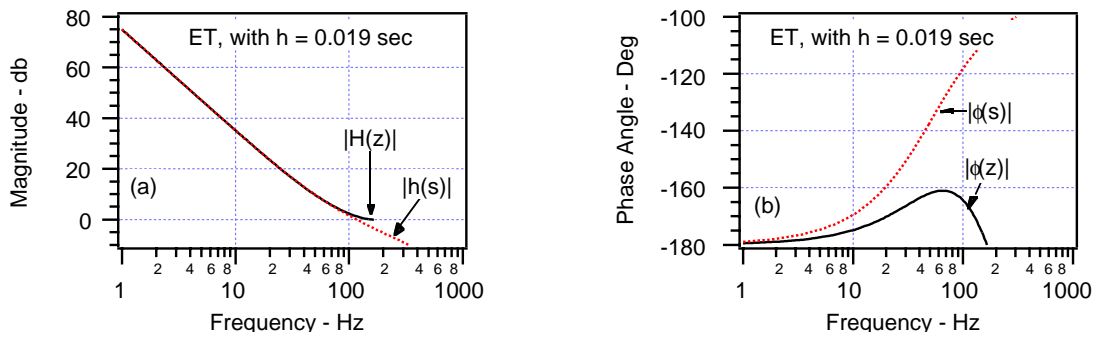


Fig. A1 - Target System Performance, $h = 0.019$ sec

In Fig. A2 the velocity time response is shown to be just barely stable, and is a poor representation of the desired response of Fig. 3.

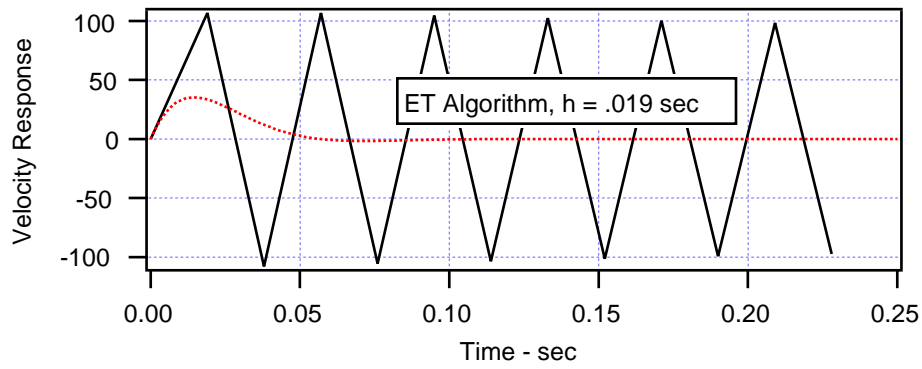


Fig. A2 - Target System Velocity, $h = 0.019$

By selecting a cycle time that is half of the maximum value, Fig. A3 is produced. The degradation in response is quite noticeable using the ET algorithm with a cycle time that is half that required for stability.

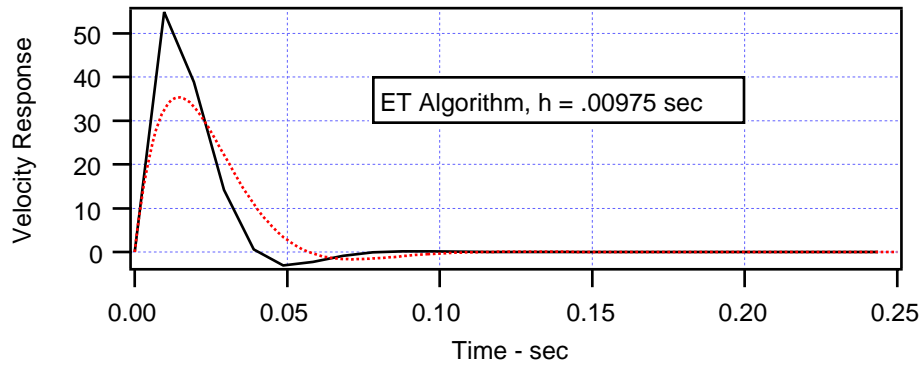


Fig. A3 - Target System Velocity, $h = 0.00975$ sec

Appendix B

Euler-Rectangular (ER)

Using Euler integration for the acceleration-to-velocity integral followed by rectangular integration for the velocity-to-position integral produces the following code fragment for a second order system,

$$\begin{aligned}\dot{y}_{k+1} &= \dot{y}_k + h\ddot{y}_k \\ y_{k+1} &= y_k + h\dot{y}_{k+1}\end{aligned}$$

where the acceleration term is redundant with the previous case (ET), and is eliminated from further consideration. This fragment may be written in z-transform notation by,

$$\begin{aligned}\dot{y}(z) &= \frac{h}{z-1} \ddot{y}(z) \\ y(z) &= \frac{hz}{z-1} \dot{y}(z)\end{aligned}$$

Hence for the Euler-Rectangular set the symbolic integrations are given by,

$$\begin{aligned}I_v(z) &= \frac{h}{z-1} \\ I_p(z) &= \frac{hz}{z-1}\end{aligned}$$

The closed-loop system for the velocity is given in z-transform notation by,

$$\frac{\dot{y}(z)}{x(z)} = \frac{\frac{h\omega_n^2}{z-1}}{1 + \frac{2\zeta\omega_n h}{z-1} + \frac{h^2\omega_n^2 z}{(z-1)^2}}$$

and in order to investigate the stability properties, we examine the open-loop function,

$$H(z) = \frac{2\zeta\omega_n h}{z-1} + \frac{\omega_n^2 h^2 z}{(z-1)^2} = \frac{\omega_n h}{(z-1)^2} [(h\omega_n + 2\zeta)z - 2\zeta]$$

which has a phase angle given by,

$$\phi = \tan^{-1} \left[\frac{2\zeta \sin \omega h}{2\zeta(1 - \cos \omega h) + \omega_n h} \right] - \pi$$

The phase margin vanishes when $\omega h = \pi$. At this frequency, where $z = -1$, the magnitude of the open-loop system is given by,

$$|H(-1)| = \frac{h\omega_n}{4}(h\omega_n + 4\zeta)$$

and the gain margin is,

$$\text{gain margin} = \frac{4}{\omega_n h(\omega_n h + 4\zeta)}$$

At the point of instability this is unity, such that

$$\omega_n h = 2(\sqrt{1 + \zeta^2} - \zeta)$$

Therefore, the cycle time must conform to the inequality,

$$h < \frac{2(\sqrt{1 + \zeta^2} - \zeta)}{\omega_n}$$

Hence, using the given damping and frequency parameters of the target system, the Euler-Rectangular scheme is unstable for cycle times above 0.0138 seconds. At this cycle time, the magnitude and phase are shown in Figs. B1(a) and B1(b). Considerable deterioration is shown in phase, as compared to the desired phase of Fig. 4(b).

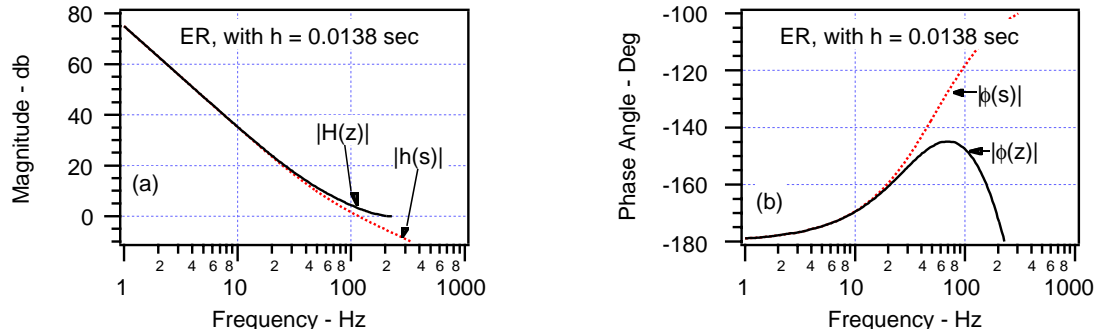


Fig. B1 - Target System Performance, $h = 0.0138$ sec

In Fig. B2 the velocity time response is shown to be just barely stable, and is a poor representation of the desired response of Fig. 3.

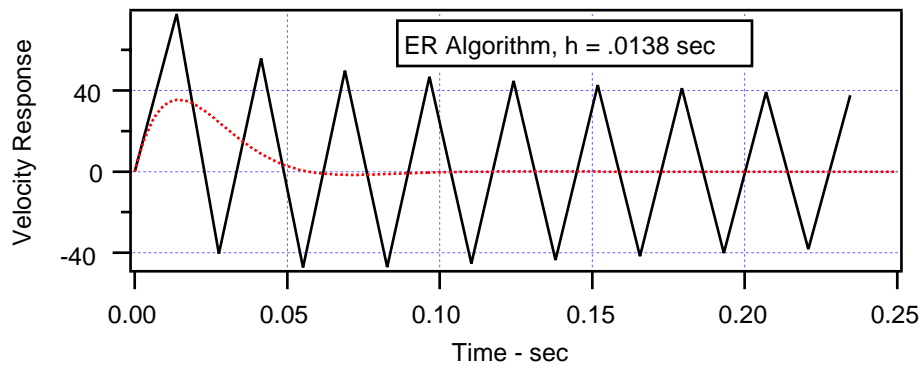


Fig. B2 - Target System Velocity, $h = 0.0138$ sec

By selecting a cycle time that is half of the maximum value, Fig. B3 is produced. The response is not too bad using the ER algorithm with a cycle time that is half that required for stability.

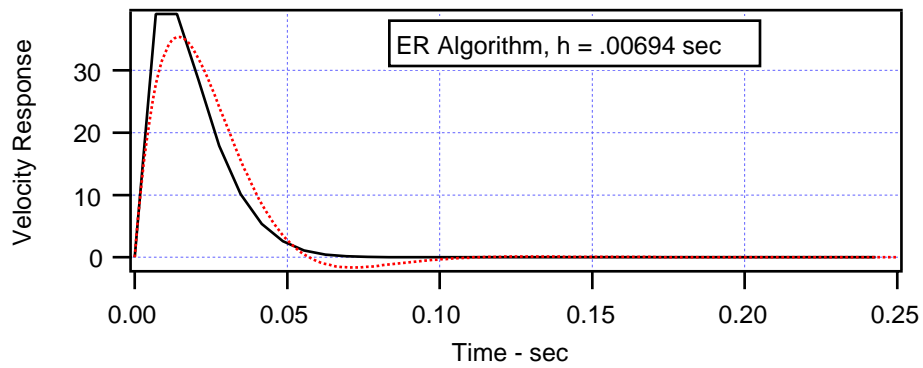


Fig. B3 - Target System Velocity, $h = 0.00694$ sec

Appendix C

Trapezoidal - Trapezoidal (TT)

Using advanced trapezoidal integration for the acceleration-to-velocity integral followed by trapezoidal integration for the velocity-to-position integral produces the following code fragment for a second order system,

$$\begin{aligned}\dot{y}_{k+1} &= \dot{y}_k + \frac{h}{2}(\ddot{y}_k + \ddot{y}_{k-1}) \\ y_{k+1} &= y_k + \frac{h}{2}(\dot{y}_{k+1} + \dot{y}_k)\end{aligned}$$

Note that the first trapezoidal process must assume an advance (explicit integration). Thus, it is not strictly “trapezoidal integration,” but could possibly be called “advancing trapezoidal”. This fragment may be written in z-transform notation by,

$$\begin{aligned}\dot{y}(z) &= \frac{h(z+1)}{2z(z-1)}\ddot{y}(z) \\ y(z) &= \frac{h(z+1)}{2(z-1)}\dot{y}(z)\end{aligned}$$

Hence, for the Trapezoidal-Trapezoidal set, the symbolic integrations are given by,

$$\begin{aligned}I_v(z) &= \frac{h(z+1)}{2z(z-1)} \\ I_p(z) &= \frac{h(z+1)}{2(z-1)}\end{aligned}$$

The closed-loop system for the velocity is given in z-transform notation by,

$$\frac{\dot{y}(z)}{x(z)} = \frac{\frac{h\omega_n^2(z+1)}{2z(z-1)}}{1 + \frac{\zeta\omega_n h(z+1)}{z(z-1)} + \frac{h^2\omega_n^2(z+1)^2}{4z(z-1)^2}}$$

and in order to investigate the stability properties, we examine the open-loop function,

$$H(z) = \frac{\zeta\omega_n h(z+1)}{z(z-1)} + \frac{\omega_n^2 h^2(z+1)^2}{4z(z-1)^2} = \frac{\omega_n h(z+1)}{4z(z-1)^2} [(h\omega_n + 4\zeta)z + h\omega_n - 4\zeta]$$

which has a phase angle given by,

$$\phi = \tan^{-1} \left\{ \frac{-\sin \omega h [\omega_n h + (\omega_n h - 4\zeta) \cos \omega h]}{(1 + \cos \omega h) [4\zeta + (\omega_n h - 4\zeta) \cos \omega h]} \right\} - \pi$$

The phase margin vanishes when,

$$\cos \omega h = \frac{\omega_n h}{4\zeta - \omega_n h}$$

Substituting this into the expression for $|H(z)|^{-1} = 1$, which is the point at which the system becomes unstable, produces,

$$\omega_n^2 h^2 \zeta - 2(1 + 2\zeta^2)\omega_n h + 4\zeta^2 = 0$$

with solution,

$$\omega_n h = \frac{1 + 2\zeta^2 - \sqrt{1 + 4\zeta^4}}{\zeta}$$

producing a gain margin of,

$$\text{gain margin} = \frac{1 + 2\zeta^2 - \sqrt{1 + 4\zeta^4}}{\zeta \omega_n h}$$

At the point of instability this is unity. Hence, the cycle time must conform to the inequality,

$$h < \frac{1 + 2\zeta^2 - \sqrt{1 + 4\zeta^4}}{\zeta \omega_n}$$

Using the given damping and frequency parameters of the target system, the (advanced) Trapezoidal-Trapezoidal scheme is unstable for cycle times above 0.011 seconds. At this cycle time, the magnitude and phase are shown in Figs. C1(a) and C1(b). Considerable deterioration is shown in phase, as compared to the desired phase of Fig. 4(b).

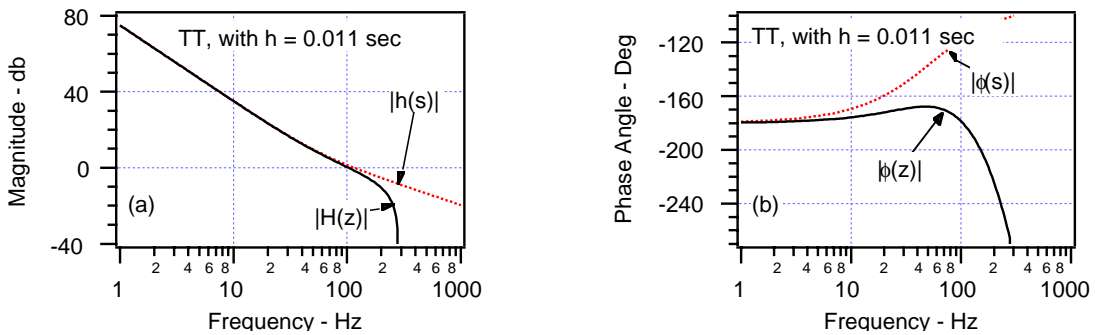


Fig. C1 - Target System Performance, $h = 0.011$ sec

In Fig. C2 the velocity time response is shown to be just barely stable, and is a poor representation of the desired response of Fig. 3.

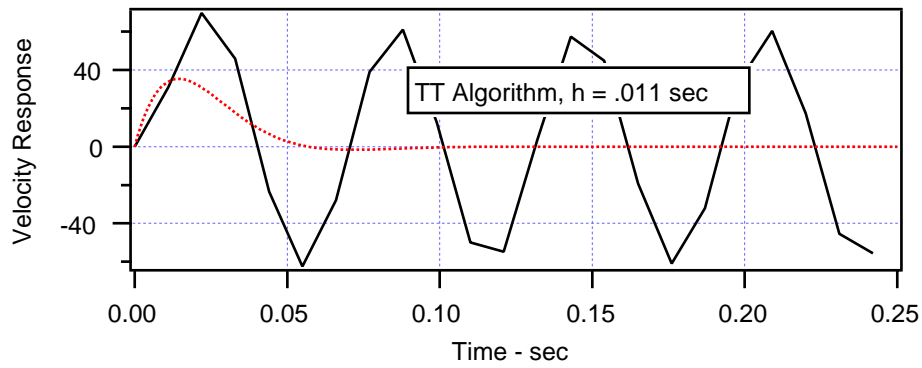


Fig. C2 - Target System Velocity, $h = 0.011$ sec

By selecting a cycle time that is half of the maximum value, Fig. C3 is produced. The response is still not very good using the TT algorithm with a cycle time that is half that required for stability.

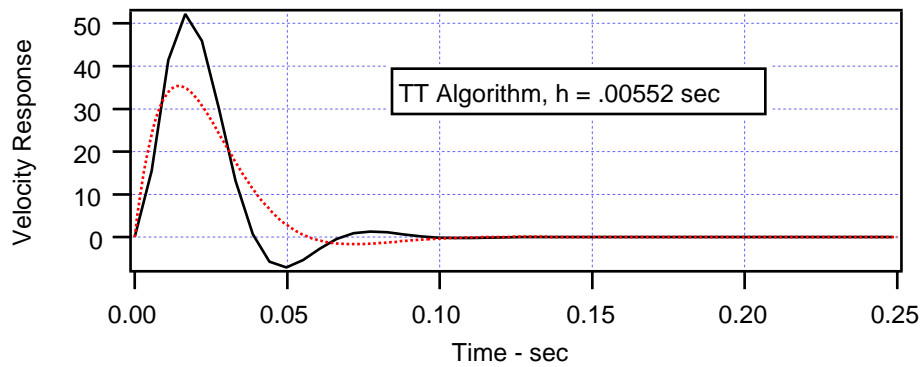


Fig. C3 - Target System Velocity, $h = 0.00552$ sec

Appendix D

Adams-Bashforth 2nd - Trapezoidal (AT)

Using the Adams-Bashforth 2nd order integration algorithm for the acceleration-to-velocity integral followed by trapezoidal integration for the velocity-to-position integral produces the following code fragment for a second order system,

$$\begin{aligned}\dot{y}_{k+1} &= \dot{y}_k + \frac{h}{2}(3\ddot{y}_k - \ddot{y}_{k-1}) \\ y_{k+1} &= y_k + \frac{h}{2}(\dot{y}_{k+1} + \dot{y}_k)\end{aligned}$$

which may be written in z-transform notation by,

$$\begin{aligned}\dot{y}(z) &= \frac{h(3z-1)}{2z(z-1)}\ddot{y}(z) \\ y(z) &= \frac{h(z+1)}{2(z-1)}\dot{y}(z)\end{aligned}$$

Hence for the Adams-Trapezoidal set the symbolic integrations are given by,

$$\begin{aligned}I_v(z) &= \frac{h(3z-1)}{2z(z-1)} \\ I_p(z) &= \frac{h(z+1)}{2(z-1)}\end{aligned}$$

The closed-loop velocity system is given in z-transform notation by,

$$\frac{\dot{y}(z)}{x(z)} = \frac{\frac{h\omega_n^2(3z-1)}{2z(z-1)}}{1 + \frac{\zeta\omega_n h(3z-1)}{z(z-1)} + \frac{\omega_n^2 h^2(z+1)(3z-1)}{4z(z-1)^2}}$$

and in order to investigate the stability properties, we examine the open-loop function,

$$H(z) = \frac{\zeta\omega_n h(3z-1)}{z(z-1)} + \frac{\omega_n^2 h^2(z+1)(3z-1)}{4z(z-1)^2} = \frac{\omega_n h(3z-1)}{4z(z-1)^2} [(\omega_n h + 4\zeta)z + \omega_n h - 4\zeta]$$

which has a phase angle given by,

$$\begin{aligned}\phi &= \tan^{-1} \left\{ \frac{\sin \omega h [4\zeta(2 - \cos \omega h) - \omega_n h(1 - \cos \omega h)]}{4\zeta(1 - \cos \omega h)^2 - \omega_n h(1 + \cos \omega h)(2 - \cos \omega h)} \right\} - \pi \\ &= \tan^{-1} \left\{ \frac{\tan \frac{\omega h}{2} [8\zeta - \omega_n h - (4\zeta - \omega_n h) \cos \omega h]}{4\zeta - 2\omega_n h + (\omega_n h - 4\zeta) \cos \omega h} \right\} - \pi\end{aligned}$$

As $\omega h \rightarrow \pi$ (the Nyquist frequency) the phase margin vanishes. At this frequency, where $z = -1$, the system magnitude is given by,

$$|H(-1)| = 2\zeta\omega_n h$$

and the system is unstable if $|H(z)|$ is outside the unit circle. Thus, for stability the cycle time must conform to the inequality,

$$h < \frac{1}{2\zeta\omega_n}$$

The phase margin also vanishes if

$$\cos \omega h = \frac{8\zeta - \omega_n h}{4\zeta - \omega_n h}$$

From a consideration of the possible values of the cosine, this only occurs if,

$$\zeta \leq \frac{\omega_n h}{6}$$

Hence if $6\zeta \leq \omega_n h$, the gain margin vanishes ($|H(z)| > 1$) before $\omega h \rightarrow \pi$. The magnitude of the open-loop transfer function is given by,

$$\begin{aligned} |H(z)| &= \left| \frac{\omega_n h(3z-1)}{4z(z-1)^2} [(\omega_n h + 4\zeta)z + \omega_n h - 4\zeta] \right| \\ &= \frac{\omega_n h}{4(1 - \cos \omega h)} \sqrt{(5 - 3\cos \omega h)[\omega_n^2 h^2 + 16\zeta^2 + (\omega_n^2 h^2 - 16\zeta^2)\cos \omega h]} \end{aligned}$$

and evaluating at the cosine value for zero phase margin,

$$\left| H\left(\cos \omega h = \frac{8\zeta - \omega_n h}{4\zeta - \omega_n h}\right) \right| = \frac{\omega_n h(\omega_n h - 4\zeta)(\omega_n h + 2\zeta)}{8\zeta}$$

because $6\zeta \leq \omega_n h$. Evaluating at the condition of equality, note that,

$$|H(\omega_n h = 6\zeta)| \geq \frac{\omega_n^2 h^2}{3} = 12\zeta^2$$

Hence, the additional limitation occurs at or below $\zeta = 1/\sqrt{12}$ (where $\omega_n h = \sqrt{3}$). For stability in this region we must have,

$$\zeta \geq \frac{\sqrt{9\omega_n^4 h^4 + 8\omega_n^2 h^2 + 16} - 4 - \omega_n^2 h^2}{8\omega_n h}$$

These relationships produce a piecewise continuous curve, where the inequalities required for a stable Adams-Trapezoidal algorithm are expressed in terms of the duty cycle:

$$\zeta \geq \begin{cases} \frac{\sqrt{9\omega_n^4 h^4 + 8\omega_n^2 h^2 + 16} - 4 - \omega_n^2 h^2}{8\omega_n h} & \zeta < 1/\sqrt{12} \\ \frac{1}{2\omega_n h} & \zeta \geq 1/\sqrt{12} \end{cases}$$

Hence, using the given damping and frequency parameters of the target system, the Adams-Trapezoidal scheme is unstable for cycle times above 0.0095 seconds. At this cycle time, the magnitude and phase are shown in Figs. D1(a) and D1(b). Considerable deterioration is shown in phase, as compared to the desired phase of Fig. 4(b).

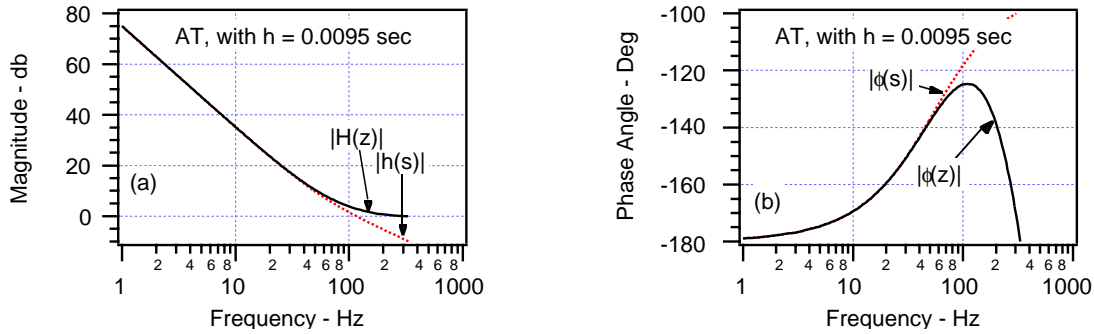


Fig. D1 - Target System Performance, $h = 0.0095$ sec

In Fig. D2 the velocity time response is shown to be just barely stable, and is a poor representation of the desired response of Fig. 3.

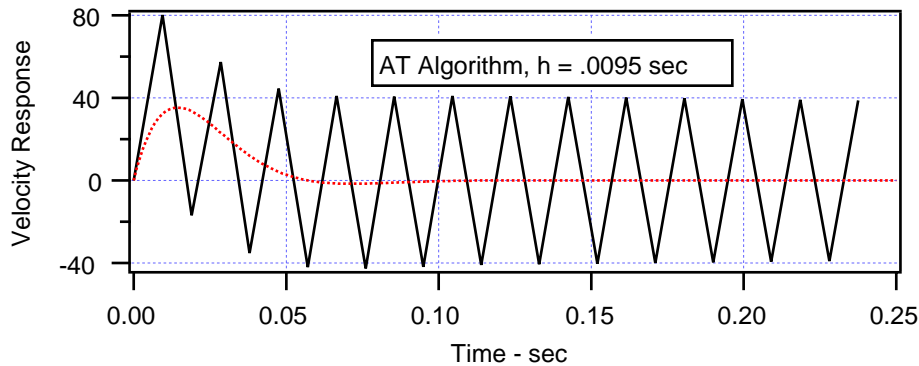


Fig. D2 - Target System Velocity, $h = 0.0095$ sec

By selecting a cycle time that is half of the maximum value, Fig. D3 is produced. The response is fairly good using the AT algorithm with a cycle time that is half that required for stability.

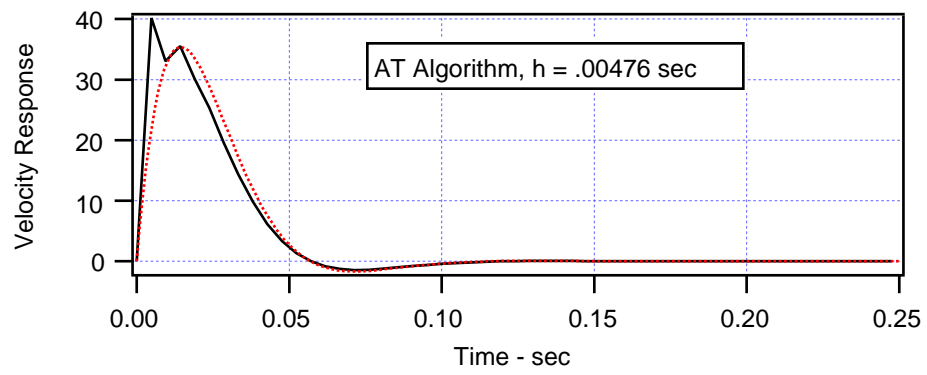


Fig. D3 - Target System Velocity, $h = 0.00476$ sec

Appendix E

Adams-Bashforth 2nd - Rectangular (AR)

Using the Adams-Bashforth 2nd order integration algorithm for the acceleration-to-velocity integral followed by rectangular integration for the velocity-to-position integral produces the following code fragment for a second order system,

$$\begin{aligned}\dot{y}_{k+1} &= \dot{y}_k + \frac{h}{2}(3\ddot{y}_k - \ddot{y}_{k-1}) \\ y_{k+1} &= y_k + h\dot{y}_{k+1}\end{aligned}$$

which may be written in z-transform notation by,

$$\begin{aligned}\dot{y}(z) &= \frac{h(3z-1)}{2z(z-1)}\ddot{y}(z) \\ y(z) &= \frac{hz}{z-1}\dot{y}(z)\end{aligned}$$

Hence for the Adams-Rectangular set the symbolic integrations are given by,

$$\begin{aligned}I_v(z) &= \frac{h(3z-1)}{2z(z-1)} \\ I_p(z) &= \frac{hz}{z-1}\end{aligned}$$

The closed-loop velocity system is given in z-transform notation by,

$$\frac{\dot{y}(z)}{x(z)} = \frac{\frac{h\omega_n^2(3z-1)}{2z(z-1)}}{1 + \frac{\zeta\omega_n h(3z-1)}{z(z-1)} + \frac{\omega_n^2 h^2 z(3z-1)}{2(z-1)^2}}$$

and in order to investigate the stability properties, we examine the open-loop function,

$$H(z) = \frac{\zeta\omega_n h(3z-1)}{z(z-1)} + \frac{\omega_n^2 h^2 z(3z-1)}{2z(z-1)^2} = \frac{\omega_n h(3z-1)}{2z(z-1)^2} [(\omega_n h + 2\zeta)z - 2\zeta]$$

which has a phase angle given by,

$$\phi = \tan^{-1} \left\{ \frac{\sin \omega h [\omega_n h + 4\zeta(2 - \cos \omega h)]}{4\zeta(1 - \cos \omega h)^2 + \omega_n h(3 - \cos \omega h)} \right\} - \pi$$

As $\omega h \rightarrow \pi$ (the Nyquist frequency), the phase margin vanishes. At this frequency, where $z = -1$, the system magnitude is given by,

$$|H(-1)| = \frac{\omega_n h}{2} (\omega_n h + 4\zeta)$$

$|H(z)|^{-1} = 1$ is the point at which the system becomes unstable. Evaluating at the point of instability, this relationship produces the second order equation,

$$(\omega_n h)^2 + 4\zeta(\omega_n h) - 2 = 0$$

which has only one positive solution. Hence, for stability the cycle time must conform to the following inequality,

$$h < \frac{2\left(\sqrt{\zeta^2 + \frac{1}{2}} - \zeta\right)}{\omega_n}$$

Using the given damping and frequency parameters of the target system, the Adams-Rectangular scheme is unstable for cycle times above 0.0078 seconds.

At this cycle time, the magnitude and phase are shown in Figs. E1(a) and E1(b). Considerable deterioration is shown in phase, as compared to the desired phase of Fig. 4(b).

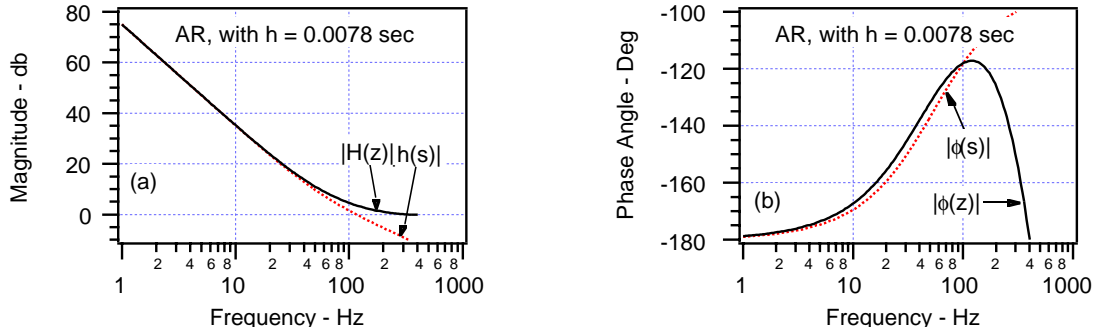


Fig. E1 - Target System Performance, $h = 0.0078$ sec

In Fig. E2 the velocity time response is shown to be just barely stable, and is a poor representation of the desired response of Fig. 3.

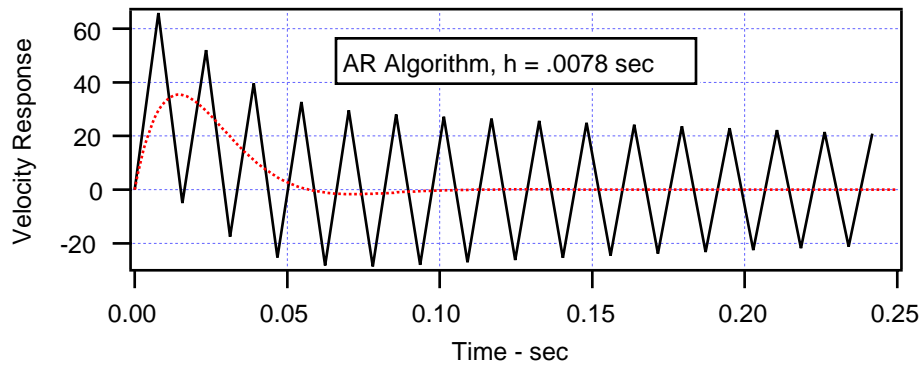


Fig. E2 - Target System Velocity, $h = 0.0078$ sec

By selecting a cycle time that is half of the maximum value, Fig. E3 is produced. The response is pretty good using the ER algorithm with a cycle time that is half that required for stability.

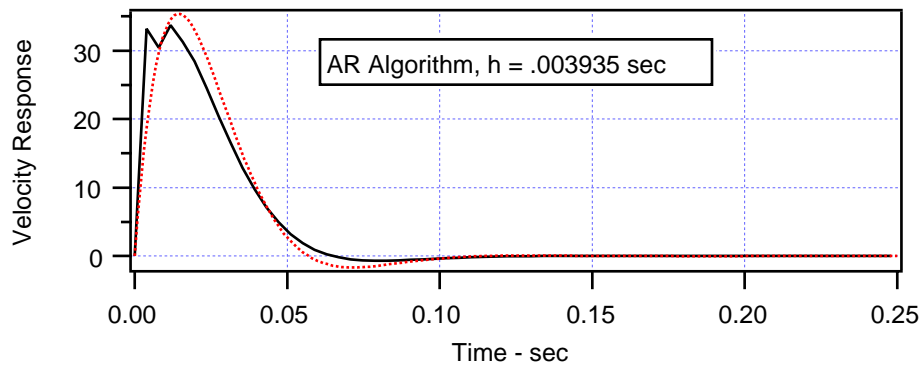


Fig. E3 - Target System Velocity, $h = 0.003935$ sec